

## Potentials, band structures, and Fermi surfaces in the noble metals

O. Jepsen

*Nordita, DK-2100 Copenhagen, Denmark  
and Max-Planck-Institut für Festkörperforschung, D-7000 Stuttgart 80, Federal Republic of Germany*

D. Glötzel

*Kernforschungsanlage Jülich, D-5170 Jülich, Federal Republic of Germany  
and Max-Planck-Institut für Festkörperforschung, D-7000 Stuttgart 80, Federal Republic of Germany*

A. R. Mackintosh

*H. C. Ørsted Institute, University of Copenhagen, DK-2100 Denmark*

(Received 2 June 1980)

We have calculated the electronic energy-band structures of the noble metals—Cu, Ag, and Au—by the linear-augmented-plane-wave (LAPW) method. The potentials were constructed using the local approximation to the density-functional formalism and calculated self-consistently by the atomic-sphere approximation to the linear-muffin-tin-orbital (LMTO) method. Relativistic band shifts were included but spin-orbit coupling was neglected. The band structures are analyzed in terms of canonical bands, which describe the dependence on the crystal structure, and potential parameters. The latter are derived from the potential in a single atomic cell and specify the positions and widths of the various bands, and hence the degree of hybridization between them. The effect of the relative band positions on the anisotropy and neck radius of the Fermi surface is discussed. Empirical logarithmic derivatives deduced from de Haas-van Alphen measurements are used to evaluate a number of different potentials, and we find that our potentials account for the Fermi surfaces comparatively satisfactorily. It is emphasized that relativistic band shifts are significant for all three metals, and that the neck radius is not, in itself, a good criterion for evaluating how well a potential reproduces the overall shape of the experimental Fermi surface. Optical measurements of excitation energies are compared with calculated differences in band energies and it is discovered that no existing *a priori* potential is able to account satisfactorily for all of the experimental evidence. The main discrepancies are due to the difficulty of placing the *d* bands consistently, and it is suggested that many-body corrections to the excitation energies may be particularly important when *d* electrons are involved.

### I. INTRODUCTION

The understanding of the electronic structure of the noble metals Cu, Ag, and Au is a classic problem in solid-state physics. The first satisfactory technique for calculating energy-band structures for metals with *d* electrons in the conduction bands was developed by Slater.<sup>1</sup> His augmented-plane-wave (APW) method has since been used for the majority of calculations on transition metals. Chodorow<sup>2</sup> applied it to Cu, using a semiempirical potential, and determined energy eigenvalues at the symmetry points  $\Gamma$ ,  $X$ , and  $L$  of the fcc Brillouin zone, shown in Fig. 1. From these results it is possible to infer that the theoretical Fermi surface probably contacts the zone boundary near  $L$ , but it was not until the development of electronic computers allowed the calculation of the full band structure by Burdick<sup>3</sup> and Segall<sup>4</sup> that the remarkable success of Chodorow's potential, which gives Fermi surface dimensions within a few percent of the most accurate experimental values, became apparent.

It is interesting that the pioneering measurements of Justi and Scheffers<sup>5</sup> on the magnetoresistance of pure single crystals of Au clearly show, with the benefit of hindsight, that its Fermi

surface must be open. However, it was the anomalous skin-effect experiments on Cu by Pippard,<sup>6</sup> from which he deduced the first complete description of the Fermi surface for any metal, which provided the impetus for rapid progress in the study of the electronic structures of the noble metals. Although the shape which he derived differs somewhat from that later deduced from more precise experimental methods, it included the essential feature of contact with the zone boundary which

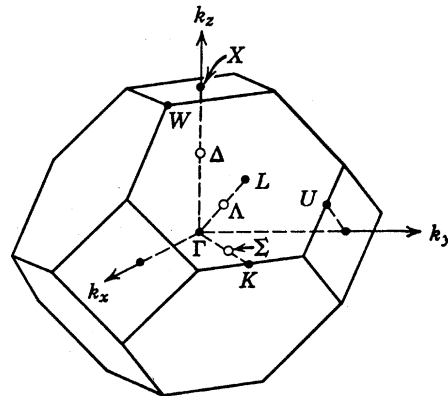


FIG. 1. Brillouin zone for the fcc structure.

gives rise to many interesting effects, especially in a magnetic field. This feature was shown to be common to all the noble metals by the de Haas-van Alphen measurements of Shoenberg,<sup>7</sup> and in the following years the Fermi surfaces were studied in great detail by a variety of methods. Successive improvements in the precision with which de Haas-van Alphen (dHvA) frequencies and amplitudes can be measured have led to the determination of the extremal areas in all three metals with a relative accuracy<sup>8</sup> of about 1 in 10<sup>6</sup>, while the effective masses have been measured<sup>9</sup> to within 0.3%.

The potentialities of electromagnetic radiation for exploring the band structure away from the Fermi level were first clearly revealed by the optical-absorption measurements of Ehrenreich and Philipp,<sup>10</sup> the photoemission experiments of Spicer and Berglund,<sup>11</sup> and the piezo-optical studies of Gerhardt.<sup>12</sup> Angle-resolved photoemission from single crystals has now been developed to the point where the energy bands may be plotted with great precision, especially in symmetry directions, as in the recent work of Knapp *et al.*<sup>13</sup> and Thiry *et al.*<sup>14</sup>

This abundance of detailed and accurate experimental information presents the challenge of explaining it by means of first-principles calculations. The computation of the electronic band structure and Fermi surface from a given potential provides no fundamental problems but, in the construction of such a one-electron potential, difficulties of both a conceptual and practical nature are encountered. The local-density theory of Hohenberg, Kohn, and Sham<sup>15</sup> provides a justification for the use of a one-electron potential in the calculation of ground-state properties, such as the Fermi surface, and a prescription for constructing it. The energy bands to which it leads are not, however, immediately applicable to the determination of optical excitation energies.

A number of such one-electron potentials have been constructed since Chodorow's pioneering work. A prescription which has met with great success in the calculation of transition-metal band structures is based upon the approximation of calculating a spherically symmetric charge distribution within the Wigner-Seitz cell by superposing atomic charge densities centered on neighboring lattice sites.<sup>16</sup> The electrostatic contribution to the potential may then be determined from Poisson's equation and the exchange and correlation treated through Slater's<sup>17</sup> local-density approximation. This non-self-consistent potential is frequently known as the standard potential. A thorough investigation of the band structures of all the noble metals using such standard potentials,

and including relativistic effects, has been carried out by Christensen.<sup>18</sup>

A modification of this procedure consists in multiplying the exchange-correlation term by a parameter  $\alpha$ , giving the so-called  $X\alpha$  potential. Janak *et al.*<sup>19</sup> used such a potential in self-consistent calculations on Cu, adjusting  $\alpha$  empirically to obtain a Fermi surface with a neck size in agreement with experiment ( $\alpha = 0.77$ ). They later<sup>20</sup> introduced another parameter, which has the effect of increasing all band energies relative to the Fermi level by 8%, in order to obtain better agreement with photoemission experiments.

The very precise data on Fermi-surface areas contain implicitly information on the crystal potential. Segall and Ham<sup>21</sup> suggested that these areas should be fitted empirically by means of a calculation in which the partial-wave phase shifts of the potential, evaluated at the Fermi level, are used as a small adjustable parameter set. This method has been extensively applied to transition metals and, in particular, Shaw *et al.*<sup>22</sup> have made a very accurate fit to the extremal areas in the noble metals with adjustable  $s$ -,  $p$ -,  $d$ -, and (for Cu)  $f$ -phase shifts in a least-squares parametrization scheme. Chen and Segall<sup>23</sup> extended this idea by parametrizing the logarithmic derivatives (equivalent to the phase shifts) over a range of energies, in order also to fit optical and photoemission data. With two parameters for each of the  $s$ - and  $p$ - and three for the  $d$ -logarithmic derivatives, they were able to obtain a very good empirical fit to the most reliable experimental information on the band structure available at the time of their work.

The principal aim of this paper is to make a critical examination of the extent to which the available experimental information on the electronic structure of the noble metals, especially Cu, can be accounted for by a one-electron band structure, and to evaluate some of the potentials which have been used in calculations. To this end, we have added yet another set to the plethora of band-structure calculations on the noble metals which already exist. We have used the potential construction which is conceptually perhaps the most satisfactory yet proposed, the scheme developed by Hedin and Lundqvist<sup>24</sup> from the local-density theory.<sup>15</sup> This local-density potential has the advantages of being self-consistent and containing no adjustable parameters, and it is furthermore susceptible to improvement in a systematic way. It has proved remarkably successful in accounting for the ground-state properties of a variety of metals.<sup>25</sup>

To anticipate our conclusion, we find that no existing band structure (including our own) can ac-

count satisfactorily both for the ground-state properties of Cu, particularly the Fermi surface, and the optical excitation energies, if these are associated with energy differences in the calculated band structure. The root of the difficulty in all the noble metals seems to lie in the positioning of the  $d$  bands. It furthermore seems questionable whether it is possible to construct from local-density theory a one-electron potential which can reconcile the different experimental results, without considering many-body corrections to the excitation energies. These conclusions, though not perhaps surprising, differ somewhat from those which may be found in some previous discussions of the electronic structure of the noble metals.

We begin in the next section by describing briefly the method which we used to calculate the energy bands, and define the parameters which characterize the crystal potentials. In Sec. III, we discuss how these potential parameters and the canonical bands may be used to construct the complete band structures from their components. The results for the three metals are presented and compared. The comparison of the theoretical and experimental Fermi surfaces, with special emphasis on Cu, is taken up in Sec. IV where we make use of a novel method<sup>26</sup> for evaluating quantitatively the success of a variety of potentials in reproducing the measured Fermi surfaces. In the following section, the excitation energies determined from optical and photoemission experiments are compared with calculated energy differences in the band structures. Finally, the principal conclusions of this work are summarized and ways by which the theoretical description of the electronic structures may be improved, to account for all of the available experimental information, are considered.

## II. METHOD OF CALCULATION

In this section, we will describe briefly the methods which we used to calculate the energy bands for the noble metals. Since these methods have been discussed extensively elsewhere,<sup>27,28</sup> we will restrict ourselves to an outline of the procedure and a description of the potential parameters used to characterize the various potentials which we will consider.

Our potentials were constructed using the local approximation of Hedin and Lundqvist<sup>24</sup> to the density-functional formalism. The one-electron potentials were calculated self-consistently using the linear muffin-tin-orbital (LMTO) method of Andersen.<sup>27</sup> In the atomic-sphere approximation (ASA) to the LMTO method, the unit cell for a

closely packed solid is approximated by a sphere of radius  $s = (3\Omega/4\pi)^{1/3}$ , where  $\Omega$  is the volume of the Wigner-Seitz atomic cell. This reduces the band-structure problem to that of finding the eigenvalues and eigenfunctions for a single atomic sphere, subject to a  $\vec{k}$ -dependent boundary condition imposed by the surroundings. The information about the crystal structure is carried by the structure-constant matrix  $S_{l,m',lm}(\vec{k})$  (where  $l$  and  $m$  are the usual angular momentum quantum numbers) which is canonical in the sense that, considered as a function of  $\vec{k}s$ , it is independent of the scale of the structure.

The spherically symmetric potential in the atomic sphere is characterized by the logarithmic-derivative functions

$$D_l(E) \equiv s\phi'_l(E, s)/\phi_l(E, s),$$

where  $\phi_l(E, s)$  are the solutions of the radial Schrödinger equations for the energy  $E$ , evaluated at the sphere boundary  $s$ . The energy dependence of a radial wave function and a logarithmic-derivative function over a range of energies about a fixed but arbitrary energy  $E_{vl}$  may be accurately described by the first few terms of a Taylor-series expansion of  $\phi_l(E, s)$ . The definition of the parameters used in such an expansion may be found in Ref. 27. In our discussion, we shall make use of the following descriptive potential parameters, which may also be derived from the expansion coefficients: The center of the  $l$  band and its square-well pseudopotential are the energies at which the logarithmic derivatives are, respectively,  $-l-1$  and  $l$ , i.e.,

$$C_l \equiv E(D_l = -l-1) \quad \text{and} \quad V_l \equiv E(D_l = l).$$

In particular,  $V_s$  is the bottom of the  $s$  band. The corresponding intrinsic band masses are

$$\mu_l \equiv [ \frac{1}{2}s^3\phi_l^2(C_l, s) ]^{-1}$$

and

$$\tau_l \equiv (2l+3) [ s^3\phi_l^2(V_l, s) ]^{-1},$$

and they are inversely proportional to the probability density at the atomic sphere, and to the width of the  $l$  band. For free electrons  $V_l = 0$  and  $\tau_l = \mu_l = 1$  for all values of  $l$  and  $s$ . The relative dimensionless band positions are given by  $\Delta_{ll'} \equiv (C_l - C_{l'})s^2$ .

The potential parameters for the noble metals in Table I were calculated self-consistently in the ASA, truncating the  $l$  expansion after  $l=3$ . Relativistic band shifts were included in the calculation, but spin-orbit coupling, which has very little influence on the Fermi surfaces, was omitted. The  $\vec{k}$ -space integrations were performed by the tetrahedron method,<sup>29</sup> using 715  $\vec{k}$  points in the

irreducible Brillouin zone, and the self-consistency iterations were continued until all energies were converged to better than 1 mRy. The values of  $E_{vl}$  were chosen at the center of gravity of the occupied parts of the  $l$ -projected density of states.

The self-consistent potentials so constructed were used in calculations of the energy bands by the linear augmented-plane-wave (LAPW) method<sup>27</sup> which is more accurate than the LMTO-ASA method. The energies near the Fermi energy were obtained with high accuracy by using values of  $E_{vl}$  close to  $E_F$ . A detailed calculation of the Fermi surface was performed for Cu using 715  $\vec{k}$  points in the irreducible zone, while the energy bands for Ag and Au were obtained along all of the symmetry lines in the zone.

TABLE I. Potential parameters for the noble metals, calculated with self-consistent local-density potentials. Energies relative to the electrostatic energy at the atomic sphere.

	Cu	Ag	Au
$Z$	29	47	79
$s$ (a.u.)	2.669	3.005	3.002
$V(s)$ (Ry)	-0.766	-0.706	-0.755
$E_v$ (Ry)			
$s$	-0.546	-0.544	-0.638
$p$	-0.404	-0.450	-0.491
$d$	-0.358	-0.508	-0.471
$f$	0.300	-0.502	-0.465
$\omega_-$ (Ry)			
$s$	0.105	0.088	0.027
$p$	0.960	0.879	0.911
$d$	0.011	0.000	0.002
$f$	3.543	3.384	3.182
$10s\Phi_-^2$ (Ry)			
$s$	3.325	2.702	2.562
$p$	3.162	2.705	2.796
$d$	0.174	0.220	0.325
$f$	3.613	2.958	2.826
$\Phi_-/\Phi_+$			
$s$	0.845	0.850	0.843
$p$	0.671	0.693	0.700
$d$	-0.028	0.056	0.088
$f$	0.535	0.556	0.544
$\langle\phi_{vl}^2\rangle^{-1/2}$ (Ry)			
$s$	4.190	3.556	3.304
$p$	5.913	5.332	5.619
$d$	0.612	0.876	0.909
$f$	11.203	9.085	8.663

### III. THE ENERGY BANDS

To comprehend the essentials of the noble-metal band structures, it is useful to start with the canonical bands for the fcc structure, shown in Fig. 2. The energy bands for the individual metals may be derived by placing, scaling, and slightly distorting the canonical bands<sup>28</sup> using the potential parameters of Table I, and allowing them to hybridize. The effect of  $d$  hybridization on the Cu band structure is illustrated by a comparison of Figs. 3 and 4. In the former,  $sp$  hybridization is included but the  $d$ -band mixing is omitted. This is accomplished by setting the hybridization blocks of the structure constants ( $l=2$  and  $l' \neq 2$ , and vice versa) equal to zero in the LMTO method. The radius  $k_s$  of the free-electron sphere is shown in the [100] and [111] directions in the figure and it is apparent that, without  $d$  hybridization, the Fermi surface of Cu would be almost spherical. If we consider only the  $s$  and  $p$  bands, a parameter which indicates the sphericity of the Fermi surface, taking into account that a uniform scaling of the bands does not alter its shape, is

$$\beta \equiv (V_p - V_s) s^2 (\tau_s \tau_p)^{1/2}.$$

$\beta = 0$  for the free electron gas, and the values for the noble metals are given in Table II. For comparison, calculations with the standard potential<sup>28</sup> give  $\beta = -0.10$  and  $0.15$  for, respectively, Na and K, whose Fermi surfaces are close to being perfect spheres. We can therefore conclude that, in the absence of  $d$  hybridization, the hypothetical Fermi surface of Cu would be almost spherical,

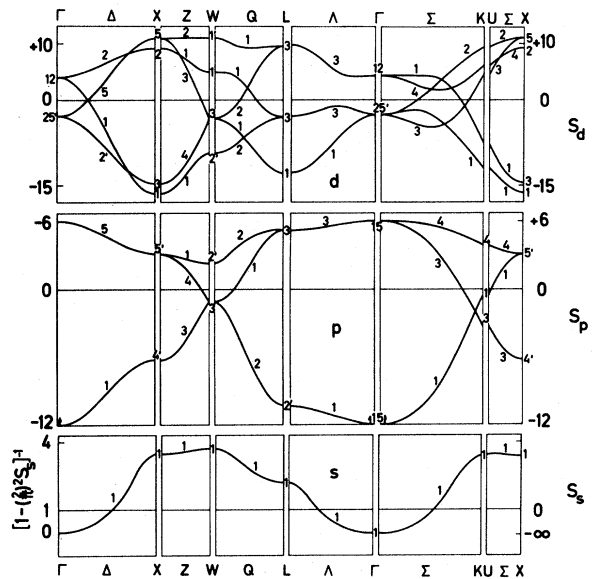


FIG. 2. Unhybridized canonical bands for the fcc structure.

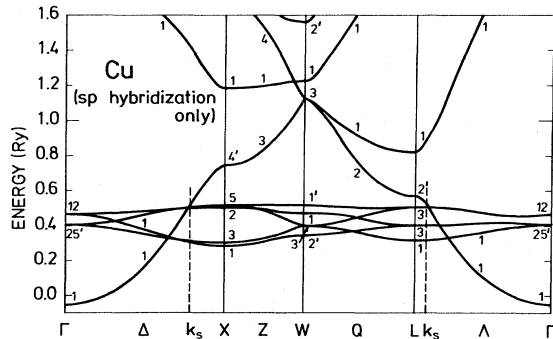


FIG. 3. Band structure of Cu when hybridization between the  $sp$  bands and the  $d$  bands is omitted.  $k_s$  is the radius of the free-electron sphere.

while that of Ag would be somewhat distorted and that of Au substantially distorted. We shall return to the question of the distortion of the Fermi surfaces in the next section.

As may be seen in Fig. 4, the  $d$  hybridization affects the band structure of Cu profoundly. Strong hybridization, occurring when unmixed bands of the same symmetry cross, produces energy gaps throughout the zone, and hence raises the Fermi level. Since the  $L_{2'}$  level is little affected by hybridization, being very slightly depressed by an admixture of a high-lying  $4f$  level, this increase in  $E_F$  results in the formation of the neck in the Fermi surface near  $L$ . Weak hybridization with the  $d$  band also causes substantial shifts in most of the  $sp$  bands. Of particular interest is the raising of the  $L_1$  level, which is predominantly  $s$ -like with a small  $d$  admixture, and the resulting increase in the  $L_1-L_{2'}$  separation (the " $L$  gap") which, as we shall see, can be accurately measured.

The band structures along the symmetry lines in the zone are shown for Cu, Ag, and Au, respectively, in Figs. 4, 5, and 6, and the eigenvalues at symmetry points are tabulated in Table

TABLE II. Theoretical parameters for the noble metals, calculated with self-consistent local-density potentials. The values in parenthesis were calculated from standard potentials.  $N_i(E_F)$  and  $n_i$  are, respectively, the projected state densities (in states/atom Ry) at the Fermi level and numbers of occupied states per atom. For comparison, results of the free-electron (FE) model are included.

	Cu	Ag	Au	FE
$\Delta_{ps}$	6.93(6.89)	7.99(7.72)	9.29(8.86)	7.40
$\Delta_{ds}$	0.67(0.56)	-0.47(-0.91)	1.28(1.07)	17.70
$\mu_s$	0.85(0.85)	0.82(0.84)	0.87(0.91)	1
$\mu_p$	0.96(0.97)	0.82(0.90)	0.79(0.89)	1
$\mu_d$	16.2(16.9)	10.1(10.3)	6.8(7.1)	1
$\beta$	-0.14	0.27	1.18	0.00
$N_s(E_F)$	0.28	0.38	0.34	
$N_p(E_F)$	0.74	0.90	0.60	
$N_d(E_F)$	1.08	0.56	1.05	
$N_f(E_F)$	0.02	0.02	0.02	
$n_s$	0.70	0.69	0.80	
$n_p$	0.74	0.67	0.78	
$n_d$	9.50	9.56	9.28	
$n_f$	0.06	0.09	0.14	

III. The general features of the energy bands can be understood with reference to the potential parameters of Table II. The relativistic band lowering, which decreases with increasing  $l$ , causes the  $s-p$  separation to increase substantially with atomic number. Although the  $sp$  bands resemble those for free electrons, their masses are significantly less than one. The  $d$ -band positions reflect the atomic  $d$ -energy levels, being relatively low in Ag, while the  $d$  masses decrease as the principal quantum number increases.

The density of states  $N(E_F)$  for Cu is shown in Fig. 7. Although the high peaks associated with the  $d$  bands fall well below the Fermi level, hybridization gives rise to a large  $d$  contribution to the state density at  $E_F$ , even for Ag, as shown in Table II. Concomitantly, the  $d$  states are incom-

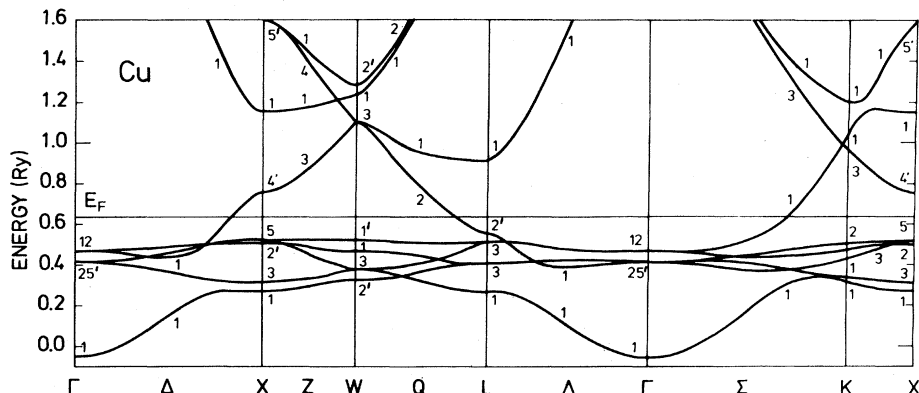


FIG. 4. Energy-band structure of Cu.

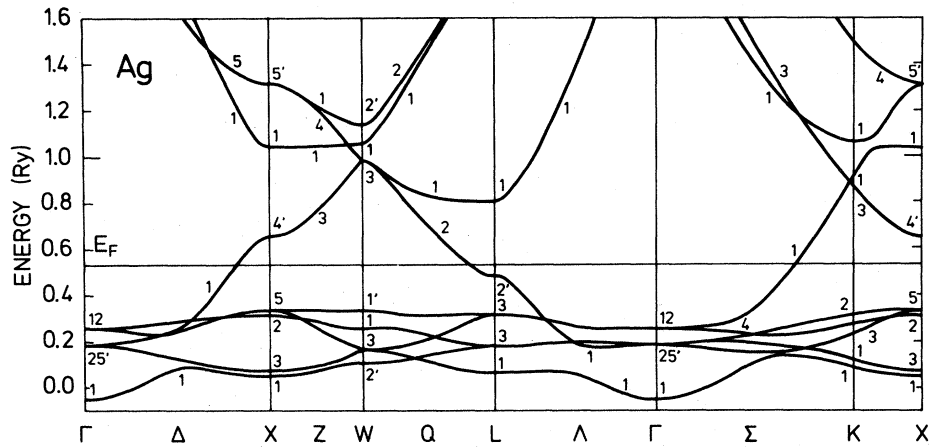


FIG. 5. Relativistic band structure of Ag neglecting spin-orbit coupling.

pletely filled, and there is a substantial fraction of a  $d$  hole per atom in all three metals.

#### IV. FERMI SURFACES

The Fermi surfaces in the noble metals may be roughly characterized by two parameters, the radius  $k_N$  of the neck and an anisotropy parameter

$$A = k_F[100]/k_F[110].$$

The values of these parameters deduced from experiment<sup>30</sup> and calculated with standard<sup>18</sup> and local-density potentials are given in Table IV. Since we only calculated energy eigenvalues along symmetry directions for Au and Ag it was necessary to estimate  $E_F$  by comparing experimental<sup>30</sup> and theoretical Fermi-surface dimensions. The Fermi level was taken as the average of the energies for which the theoretical  $k_F[100]$  and  $k_F[110]$  coincide with the experimental values. Since, as we shall see, our potentials are rather successful in reproducing the Fermi surface, this

estimate could be made with an error of less than about 5 mRy. In any case,  $A$  is very insensitive to the exact value of  $E_F$ , since the bands are accurately linear over the energy range within which it lies.

The Fermi-surface anisotropy  $A$  is increased either by the enhanced  $d$  hybridization at  $E_F$  resulting from an increase in  $\Delta_{ds}$ , or by increasing  $\Delta_{ps}$  (or rather  $\beta$ ) above the free-electron value. The distortion of the Cu Fermi surface is almost entirely due to  $d$  hybridization, which is less important in Ag because of the position of the  $d$  bands. In Au, where the  $d$  bands lie closest to the Fermi level and the relativistic lowering of the  $s$  band is greatest, the anisotropy is also greatest. The neck size is increased by increasing  $\Delta_{ds}$  or reducing  $\Delta_{ps}$ , both of which tend to raise  $E_F$  relative to the  $p$ -like  $L_2'$  level. The Ag neck is smaller than that of Cu, both because of the relativistic shift of the  $s$  band and the low-lying  $d$  bands, while the Au neck size is comparable to that of Cu, despite the large relativistic shift, because

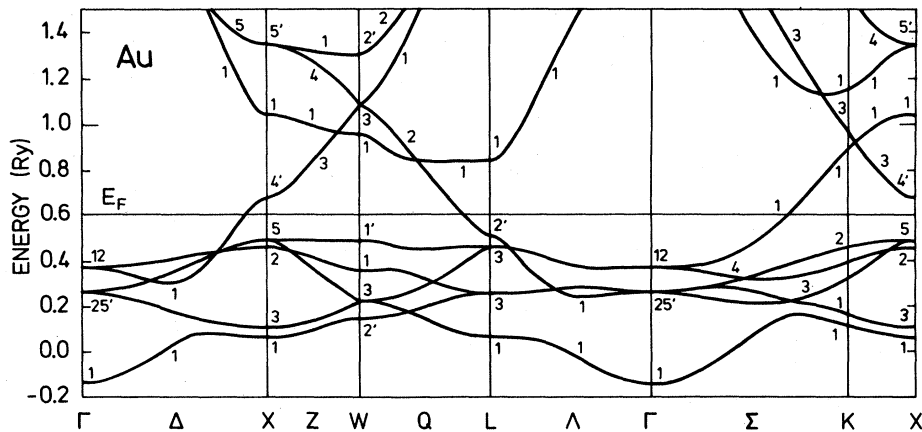


FIG. 6. Relativistic band structure of Au neglecting spin-orbit coupling.

TABLE III. Calculated energies at symmetry points relative to the muffin-tin zero, in millirydbergs, in the noble metals.

	$\Gamma$	X	W	L	K	
Cu	-52	273	325	270	320	
	$E_F = 636$	414	317	378	409	339
		414	509	378	409	432
	414	523	466	512	478	
	469	523	523	512	511	
	469	758	1103	555	962	
		1155	1103	915	1051	
	1600	1236		1204		
		1600	1285			
Ag	-52	49	106	64	87	
	185	73	163	180	121	
	$E_F = 530$	185	315	163	180	237
		185	336	258	319	274
	259	336	336	319	315	
	259	655	986	487	860	
		1041	986	809	922	
	1319	1055		1066		
	1319	1140				
Au	-139	66	149	65	120	
	266	109	228	258	169	
	$E_F = 610$	266	462	228	258	327
		266	494	361	468	394
	375	494	494	468	460	
	375	684	962	511	893	
		1046	1087	844	964	
	1346	1087		1159		
	1346	1305				

the  $d$  bands lie close to  $E_F$ .

We have used the empirical phase shifts deduced by Shaw *et al.*<sup>22</sup> from dHvA data to make a more quantitative evaluation of a number of different potentials. Because of the insensitivity of the energy bands to the interstitial regions of the muffin-tin potential, they were able to obtain equally good fits to the experimental results for a large range of assumed Fermi energies. We have converted their phase shifts to logarithmic deriva-

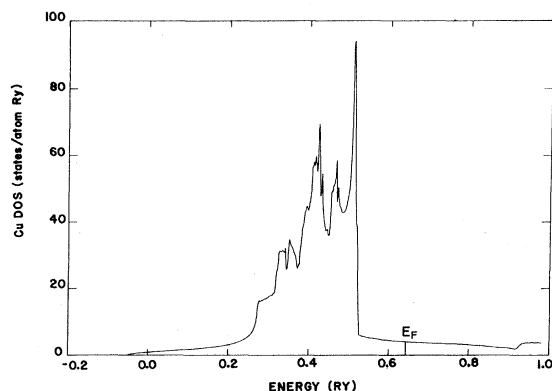


FIG. 7. Density of states for Cu.

TABLE IV. Fermi-surface anisotropy and neck radii in the noble metals.  $E$  denotes the experimental values and  $L$  and  $S$  the results of calculations based on, respectively, local density and standard potentials.

	Cu	Ag	Au
$A \equiv k_F[100]/k_F[110]$	1.11( $E$ )	1.09( $E$ )	1.20( $E$ )
	1.13( $L$ )	1.11( $L$ )	1.21( $L$ )
	1.10( $S$ )	1.06( $S$ )	1.14( $S$ )
$k_N/k_S$	0.189( $E$ )	0.136( $E$ )	0.179( $E$ )
	0.21( $L$ )	0.17( $L$ )	0.19( $L$ )
	0.20( $S$ )	0.10( $S$ )	0.16( $S$ )

tives at the atomic sphere and plotted them as a function of the assumed  $E_F$ , relative to the muffin-tin zero, in Fig. 8. We have also calculated  $D_i(E)$  as a function of energy for several potentials and plotted them on the same figure. They are:  $C(U)$ —Chodorow's potential;  $C(R)$ —Chodorow's potential with relativistic band shifts;  $S(R)$ —the standard potential;  $X(U)$ —the self-consistent  $X\alpha$  potential of Janak *et al.*<sup>19</sup>;  $L(U)$ —our nonrelativistic self-consistent local-density potential;  $L(R)$ —our relativistic local-density potential. The last three of these are self-consistent and  $R$  and  $U$  indicate whether relativistic band shifts have been included or not.

In order that a given potential should reproduce the experimental Fermi surface precisely, the

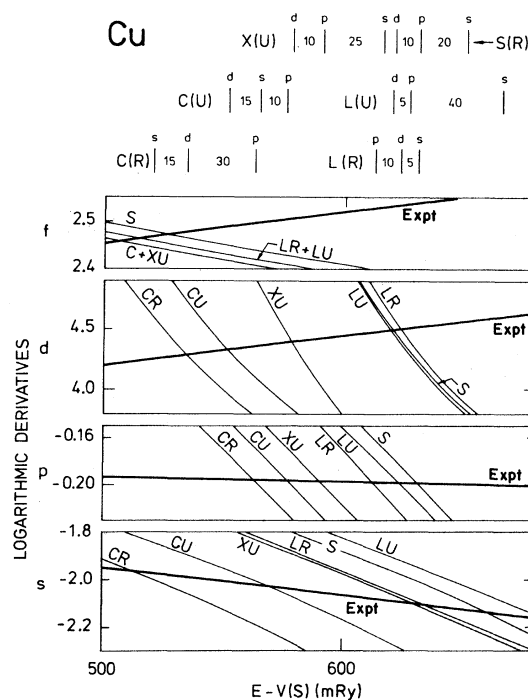


FIG. 8. Experimental and calculated logarithmic derivatives for Cu. The labeling is explained in the text.

logarithmic derivatives derived from it must cut the experimental curves at the same energy, which is then the calculated Fermi energy. The extent to which they do so is therefore a measure of the success of the potential in reproducing the experimental measurements.<sup>26</sup> The Fermi surface is relatively insensitive to the  $f$ -logarithmic derivative, and a satisfactory fit can be obtained without including it, as in Ag and Au which we discuss later. We therefore ignore it in our comparison, apart from noting that none of the calculated values agree well with the experimental values, probably because the latter implicitly include higher  $l$  values, and therefore do not represent the  $f$ -wave contribution alone.

At the top of Fig. 8, we have indicated, for each potential, energies pertaining to the  $s$ -,  $p$ -, and  $d$ -logarithmic derivatives. Since the density of states at  $E_F$  is predominantly  $d$ -like, we begin by marking the energy at which  $D_d(E)$  cuts the experimental curve. Thereafter we determine the energy shifts of the calculated  $D_s(E)$  and  $D_p(E)$  required to make them cut the appropriate experimental curves at this same energy. Thus we can conclude from Fig. 8 that, for the  $C(U)$  potential for example,  $D_s(E)$  and  $D_p(E)$  must be moved downwards in energy by, respectively,  $\delta_{sd} = 15$  mRy and  $\delta_{pd} = 25$  mRy to obtain agreement with the experimental Fermi surface. These energy shifts, which decrease as the potential is improved, provide convenient figures of merit for a given potential. It is interesting that it is essential to include relativistic effects, which give rise to a relative lowering of  $D_s(E)$  and, to a lesser extent,  $D_p(E)$ , when making comparison with experiment at this level of precision, even for the relatively light element Cu.

It is perhaps at first sight surprising that the  $X\alpha$  potential, which was adjusted to fit the experimental neck size, does not give a particularly good overall description of the Fermi surface compared with, for example, the relativistic local-density potential  $L(R)$ . The neck size is not however, in itself, an adequate figure of merit for a potential. If we neglect hybridization of the  $p$ -like  $Q_2$  band near  $L$ , the error in the neck radius is easily seen to be

$$\delta k_N = \left[ \frac{N_s(E_F)}{N(E_F)} \delta_{sd} - \left( 1 - \frac{N_p(E_F)}{N(E_F)} \right) \delta_{pd} \right] / \left( \frac{\partial \epsilon}{\partial k} \right)_{Q_2, E_F}$$

$k_N$  therefore increases with  $\delta_{sd}$  and decreases, relatively more rapidly, with  $\delta_{pd}$ . Weak hybridization with the  $d$  bands reduces substantially the effect of a given shift of the  $p$  band on the neck radius, but it is still greater than, and of opposite sign to the effect of shifting the  $s$  band. Compared

with experiment, the calculated neck radii for some of the potentials are in error by the following percentages:  $C(U)$ ,  $-2\%$ ;  $X(U)$ ,  $-\frac{1}{2}\%$ ;  $S(R)$ ,  $5\%$ ;  $L(U)$ ,  $8\%$ ;  $L(R)$ ,  $11\%$ . These deviations can be qualitatively understood, with reference to Fig. 8, by the above considerations, as can the errors in the neck radii for Ag and Au, which we consider later. The neck size for the  $X(U)$  potential is correct because the effects of  $\delta_{sd}$  and  $\delta_{pd}$  tend to cancel, while for the  $L(R)$  potential, which is otherwise superior in reproducing the shape of the Fermi surface, they add. The inclusion of relativistic effects has little influence on the neck size, because the effect of the decrease in  $\delta_{sd}$  is approximately cancelled by that of the (smaller) decrease in  $\delta_{pd}$ . We conclude that the neck radius is so sensitive to the band parameters that it may be rather poorly reproduced by a potential which gives an otherwise good account of the Fermi surface and, conversely, the prediction of the correct  $k_N$  is not, in itself, a sufficient condition for a satisfactory potential.

We have used our calculated energy eigenvalues for Cu to construct the Fermi surface, sections of which are compared with those deduced from the dHvA effect<sup>30</sup> in Fig. 9. As may be seen, the agreement is very satisfactory, except in the vicinity of the neck. Compared with experiment, the calculated belly areas in the (100) and (111) planes are, respectively, 0.26% too large and 0.29% too small. The self-consistent  $X\alpha$  potential predicts belly areas in the (100) and (111) planes which are, respectively, 1.9% and 0.2% too small.<sup>19</sup> Since the experimental (100) area is roughly 3% larger than the (111) area, the  $X\alpha$  potential underestimates the Fermi-surface anisotropy,

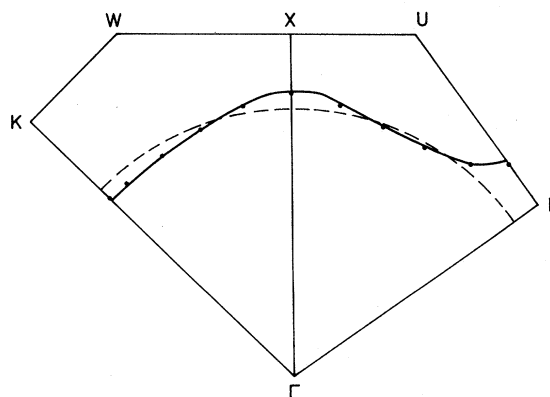


FIG. 9. Sections of the Fermi surface of Cu in the (100) and (110) planes. The full line depicts the calculated surface and the points are deduced from de Haas-van Alphen measurements. The dashed line is the free-electron sphere.

while our local-density potential slightly overestimates it.

We have carried out a similar analysis of the logarithmic derivatives derived from the standard and local-density potentials in Ag and Au, with the results shown in Figs. 10 and 11, respectively. From these and Fig. 8 we can conclude that, for both potentials,  $D_p(E)$  lies somewhat too low in energy relative to  $D_s(E)$ , in the vicinity of the Fermi level, in all three noble metals. The major difference between them is that, whereas the local-density potential leads to  $D_d(E)$  which cut the experimental curves between the energies at which  $D_s(E)$  and  $D_p(E)$  do so, and therefore reproduce the shape of the Fermi surface fairly well, the  $d$ -logarithmic derivatives calculated from the standard potential lie much too low in energy in all cases, and the calculated Fermi-surface anisotropy is therefore too small. This feature also accounts for the fact that the neck sizes are too small in both Ag and Au, as shown in Table IV. In contrast, the neck radii are too big in the calculations with the local-density potential, in Ag primarily because  $\delta_{pd}$  is negative and in Au because  $\delta_{sd}$  is positive.

#### V. OPTICAL AND PHOTOEMISSION SPECTRA

Experiments with electromagnetic radiation can give detailed results on electronic energy levels

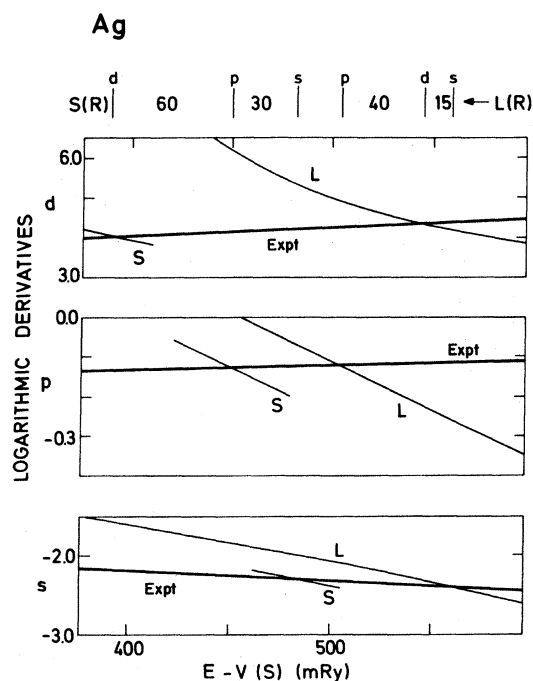


FIG. 10. Experimental and calculated logarithmic derivatives for Ag.

away from the Fermi energy. Structure in the imaginary part of the optical dielectric function  $\epsilon_2(\omega)$  can give useful information, but single-crystal piezo-optical measurements generally allow a more precise determination of energy differences at points of high symmetry within the zone. We shall find particularly useful the analysis of such data by Chen and Segall,<sup>31</sup> from which the  $L$  gap and the interband-absorption energy  $E_F - X_5$  (or  $X_{7+}$  if spin-orbit coupling is taken into account) may be accurately determined for all three metals. Finally, angular-resolved photoemission from single crystals is a very powerful technique which can yield energy bands throughout the zone. We will primarily be interested in the information which can be obtained therefrom on the widths of the  $d$  bands.

In Table V, we show the values obtained from experiment for the  $L$  gap, and the position of the top of the  $d$  band and its width, together with the results from a number of calculations. We note that spin-orbit coupling is neglected in all the calculations on Cu, where it is very small, but included for Ag and Au. Since we did not include the spin-orbit coupling in our calculations, we have assumed splittings of our energy levels equal to those determined by Christensen.<sup>18</sup> This pro-

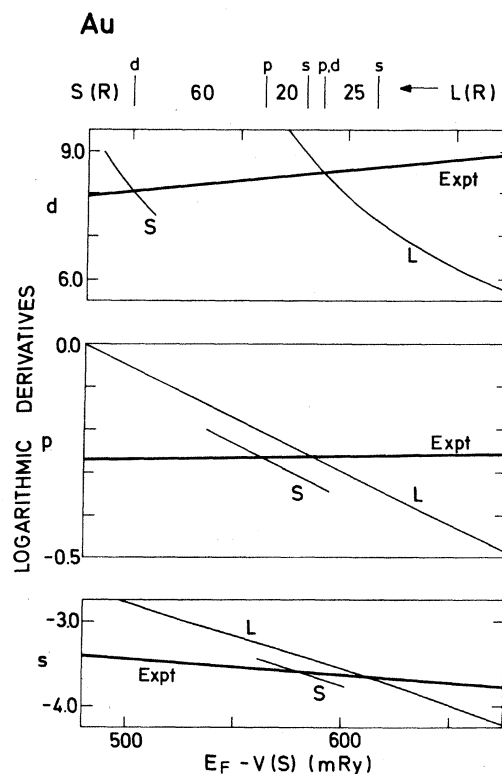


FIG. 11. Experimental and calculated logarithmic derivatives for Au.

TABLE V. Experimental and calculated energy differences, in millirydbergs, in the noble metals.

	$L_1-L_2'$	$E_F - X_5(X_{7'})$	$X_5(X_{7'}) - X_3(X_{7'})$
Cu			
Experiment	$370 \pm 10^a$	$145 \pm 10^{a,b,c}$	$180 \pm 20,^b 205 \pm 10^c$
Present work	360	113	206
Christensen <sup>d</sup>	338	118	209
Janak <i>et al.</i> <sup>e</sup>	379	143	226
Chen and Segall <sup>f</sup>	371	144	221
Ag			
Experiment	$310 \pm 10^g$	$280 \pm 10^g$	$240 \pm 10^h$
Present work	322	183	274
Christensen <sup>d</sup>	256	274	240
Chen and Segall <sup>f</sup>	311	280	257
Au			
Experiment	$335 \pm 10^i$	$115 \pm 10^i$	$400 \pm 10^j$
Present work	333	77	424
Christensen and Seraphin <sup>d</sup>	274	113	402

<sup>a</sup>Reference 12.<sup>b</sup>Reference 13.<sup>c</sup>Reference 14.<sup>d</sup>Reference 18.<sup>e</sup>Reference 20.<sup>f</sup>Reference 23.<sup>g</sup>Reference 33.<sup>h</sup>Reference 34.<sup>i</sup>Reference 37.<sup>j</sup>Reference 38.

cedure should lead to errors which are very small compared with the experimental uncertainties. We will comment on each metal in turn.

For Cu, our local-density potential gives an  $L$  gap in good agreement with experiment,<sup>12</sup> but the top of the  $d$  band apparently lies much too high. Thiry *et al.*<sup>14</sup> have determined the bottom of the  $s$  band,  $\Gamma_1$ , to lie  $630 \pm 30$  mRy below  $E_F$ , which is somewhat less than our value of 688 mRy. Knapp *et al.*<sup>13</sup> have estimated that the predominantly  $s$ -like  $X_1$  level lies 580 mRy above  $E_F$ , which is substantially greater than our value of 519 mRy, but their estimate is based principally on the secondary-emission spectrum and suffers from substantial uncertainty. The energy separation between a point on the empty  $\Delta_1$  band and  $E_F$ , which they measure to be 780 mRy, is more reliable, and is again greater than our calculated 740 mRy. However, the finite energy resolution of their apparatus would tend to give too high a value for this energy, as well as producing the kind of distortion in the spectrum which they observe, so the discrepancy may be less than it seems. It would be useful to determine the resolution function for photoemission spectrometers and systematically deconvolute the experimental data.

The calculations of Janak *et al.*,<sup>20</sup> in which the

bands are stretched by 8% to simulate many-body corrections, give an  $L$  gap and  $d$ -band top in agreement with experiment but the  $d$  bands are about 10% too broad and their  $\Gamma_1$ , which is 735 mRy below  $E_F$ , lies much too low. The standard potential places the  $d$  bands too high and the  $L$  gap is too small, compared with experiment. The empirical band structure of Chen and Segall<sup>23</sup> was fitted to the experimental data, but the estimate of Eastman and Cashion<sup>32</sup> for the  $d$ -band width, which is about 10% greater than the most recent measurements, was used.

These variations, and the predicted Fermi-surface anisotropies, can be understood with reference to the potential parameters of Table VI. These were calculated via the logarithmic derivatives from the corresponding *a priori* potentials. The empirical parametrization of the logarithmic derivatives by Chen and Segall can readily be converted into potential parameters, and are given in the table (identified as  $P$ ) for  $E_F = 588$  mRy, which is close to the value for the Chodorow potential.

The greatest variation occurs in the position of the  $d$  bands. The  $L(R)$  and  $S(R)$  potentials both give rise to relatively high-lying  $d$  bands. The hybridization with the  $s$  band, which is proportional to the geometric mean of the bandwidths, is

TABLE VI. Potential parameters for Cu from different calculations, as specified in the text.

	$\Delta_{ps}$	$\Delta_{ds}$	$\mu_s$	$\mu_p$	$\mu_d$
$C(U)$	6.92	0.29	0.86	0.92	16.1
$C(R)$	7.02	0.41	0.88	0.93	16.4
$S(R)$	6.89	0.56	0.85	0.97	16.9
$X(U)$	6.79	0.33	0.84	0.97	16.5
$L(U)$	6.82	0.43	0.83	0.96	16.3
$L(R)$	6.93	0.67	0.85	0.96	16.2
$P$	6.97	0.42	0.85	0.97	15.2
FE	7.40	17.72	1	1	1

higher for the former, for which the mass is lower, and hence the  $L$  gap and Fermi-surface anisotropy are relatively large, and in good agreement with experiment. The low-lying  $d$  bands for the  $X(U)$  potential give a smaller  $s$ - $d$  hybridization at and above  $E_F$ , so that the (uncorrected)  $L$  gap is too small, and the Fermi surface too spherical. The empirical parametrization includes  $s$ - $d$  hybridization large enough to produce agreement with experiment, despite the relatively small  $\Delta_{ds}$ , because the adopted value of  $\mu_d$  is significantly smaller than the values calculated from the *a priori* potentials.

There is less experimental evidence on Ag, and fewer calculations, but the situation seems fairly clear. The  $L$  gap and the top of the  $d$  bands are well determined from piezo-optical experiments<sup>33</sup> and their analysis,<sup>31</sup> and the  $d$ -band width from photoemission.<sup>34</sup> The  $L$  gap and Fermi-surface anisotropy are well accounted for by our local-density potential, but the  $d$  bands apparently lie too high. The standard potential yields very good agreement with experiment for both the  $d$ -band position and width, but the reduced hybridization leads to an insufficiently distorted Fermi surface and too small an  $L$  gap. As in the case of Cu, the empirical  $d$  bands of Chen and Segall<sup>23</sup> are somewhat broader than the latest experiments would indicate. It is interesting that the fine structure in the x-ray absorption near the  $K$  edge<sup>35</sup> is very well accounted for by the energy bands up to several Ry above  $E_F$  calculated from the standard potential,<sup>36</sup> if they are empirically broadened, but not shifted.

The situation for Au is very similar to that for Ag. Again our local-density potential accounts well for the experimental Fermi surface and  $L$  gap,<sup>37</sup> but not for the apparent position of the  $d$  bands. These are well described by the standard potential, but the  $L$  gap is then too small and the Fermi surface too spherical. There are some indications from photoemission experiments<sup>38</sup> that the  $d$  bands in Au might lie even lower,<sup>39</sup> but this

may be an experimental artifact due to the difficulty of locating the Fermi level precisely.<sup>34</sup>

## VI. DISCUSSION

The aim of the work presented in this paper has been to explore the extent to which calculated one-electron band structures can account for the detailed and precise experimental information which is available on the electronic structure of the noble metals. We have considered the shape of the Fermi surface, a ground-state property, and the excitation energies determined from optical and photoemission spectra.

By examining the way in which the band structures are assembled from their component parts, we have shown how the form of the Fermi surface is influenced by the relative band positions. In particular, the Fermi-surface anisotropy increases with the  $d$ -band energy because of hybridization with the states at the Fermi level, which thereby acquire a large  $d$  component, and with the  $s$ - $p$  separation, which increases with atomic number due to relativistic band shifts. The former effect also increases the size of the Fermi-surface neck, while the latter reduces it, so that the overall shape of the Fermi surface is determined by a number of factors. We have argued that the most satisfactory method of evaluating the quality of a potential in reproducing the observed Fermi surface is by using empirically derived logarithmic derivatives at  $E_F$ , such as those determined by Shaw *et al.*<sup>22</sup> By this criterion, our relativistic potential, which has the form derived by Hedin and Lundqvist<sup>24</sup> from local-density theory,<sup>15</sup> is comparatively successful for all three metals. Because of the above-mentioned competing factors, the neck radius is not, in itself, a good figure of merit for a potential. Even for Cu it is essential to include relativistic effects when comparing theory and experiment at the level of precision which is now possible. The standard potential, which is constructed from a superposition of atomic charge densities<sup>16</sup> and has been very successful in describing the electronic structure of the majority of the transition metals, is less successful for the noble metals, predicting Fermi-surface anisotropies which are consistently too small.

If the excitation energies are interpreted as energy differences in the calculated single-particle band structure, none of the *a priori* potentials which we have examined give a good quantitative account of the optical properties, even though they all agree qualitatively with the observations. Our local-density potential seems to be fairly satisfactory for the predominantly  $sp$  bands, and

in particular gives values for the ( $L_1-L_2$ ) gap which agree well with experiment, but the  $d$  bands apparently lie much too high in all three metals. Conversely, the standard potential gives  $d$  bands in good agreement with experiment, particularly for Ag and Au, but the  $L$  gaps in all cases are substantially too small.

It seems doubtful whether a local single-particle potential  $V(\vec{r})$  can be constructed which will reconcile the various experimental data within this interpretation. The principal effect of variations in such a potential is to change the relative positions of the bands. If we take Au as an extreme example, we may start with our band structure and attempt to adjust it in this way to fit the experiments. The greatest discrepancy may be removed by lowering the  $d$  band, but this will reduce both the  $L$  gap and the Fermi-surface anisotropy below what is observed. The latter may be corrected by making use of the other degree of freedom and increasing the  $s-p$  separation, but this further reduces the  $L$  gap. It seems reasonable to take the viewpoint that our local-density potential gives a good account of the ground-state properties,<sup>25</sup> including the Fermi surface, as it is constructed to do, but that the calculation of the excitation energies requires self-energy corrections which may be substantial. The uniform stretching of the bands suggested by Janak *et al.*<sup>20</sup> for this purpose has been shown by recent experimental results to be inadequate. Our calculations suggest rather that the corrections are  $l$  dependent and, perhaps not surprisingly, are largest for the relatively localized  $d$  electrons.

Chen and Segall<sup>23</sup> have demonstrated that it is possible to account for the electronic properties within a single-particle picture by parametrizing the logarithmic derivatives over a range of energies. Their published band structures are not fully in accord with the most recent measurements

of  $d$ -band widths in Cu and Ag but, since the  $E(\vec{k})$  at a particular energy depend only on the  $D_l(E)$  at that energy, it is always possible to remove any discrepancies with experiment. Their method is an ideal parametrization of a large amount of experimental data, with a small parameter set. However, as they point out, there is no immediate justification for considering the parametrized logarithmic derivatives as derivable from an  $l$ -dependent potential which may in principle be deduced from the local density, and applied to the calculation of such ground-state properties as, for example, the cohesive energy.

We conclude that further progress on this problem will probably result from a combination of more experiments, especially with angle-resolved photoemission, and an attempt to make realistic calculations of the self-energy corrections to the excitation energies. Such calculations should also provide an interpretation of the lifetimes of the excitations, recently observed by photoemission.<sup>13,14</sup> Although they have been studied more intensively than any other metals, it is apparent that the last word has not yet been said about the electronic structure of the noble metals.

#### ACKNOWLEDGMENTS

We are deeply indebted to O. Krogh Andersen for many invaluable comments during the course of this work, including the suggestion of the method which we adopted for evaluating potentials. Fruitful discussions with B. Segall and N. E. Christensen are also gratefully acknowledged. Dr. Christensen supplied us with the results of his unpublished calculations for Cu, and V. Moruzzi kindly sent a listing of his self-consistent potential. H. L. Skriver and P. E. Mackintosh provided valuable assistance with some of the calculations.

<sup>1</sup>J. C. Slater, Phys. Rev. **51**, 151 (1937).

<sup>2</sup>M. I. Chodorow, Ph.D. thesis, Massachusetts Institute of Technology, 1939 (unpublished).

<sup>3</sup>G. A. Burdick, Phys. Rev. Lett. **7**, 156 (1961).

<sup>4</sup>B. Segall, Phys. Rev. **125**, 109 (1961).

<sup>5</sup>E. Justi and H. Scheffers, Metallwirtsch. Metallwiss. Metalltech. **17**, 1359 (1938).

<sup>6</sup>A. B. Pippard, Philos. Trans. R. Soc. London Ser. A **250**, 325 (1957).

<sup>7</sup>D. Shoenberg, Philos. Trans. R. Soc. London Ser. A **255**, 85 (1962).

<sup>8</sup>P. T. Coleridge and I. M. Templeton, J. Phys. F **2**, 643 (1972).

<sup>9</sup>B. Lengeler, W. R. Wampler, R. R. Bourassa, K. Mika,

K. Winegarth, and W. Uelhoff, Phys. Rev. B **15**, 5493 (1977).

<sup>10</sup>H. Ehrenreich and H. R. Philipp, Phys. Rev. **128**, 1622 (1962).

<sup>11</sup>W. E. Spicer and C. N. Berglund, Phys. Rev. Lett. **12**, 9 (1964).

<sup>12</sup>U. Gerhardt, Phys. Rev. **172**, 651 (1968).

<sup>13</sup>J. A. Knapp, F. J. Himpsel, and D. E. Eastman, Phys. Rev. **19**, 4952 (1979).

<sup>14</sup>P. Thiry, D. Chandessris, J. Lecante, C. Guillot, R. Pinchaux, and Y. Pétroff, Phys. Rev. Lett. **43**, 82 (1979).

<sup>15</sup>P. Hohenberg and W. Kohn, Phys. Rev. **136**, B864 (1964); W. Kohn and L. J. Sham, Phys. Rev. **140**,

- A1133 (1965).
- <sup>16</sup>L. M. Mattheiss, *Phys. Rev.* **133**, A1399 (1964).
- <sup>17</sup>J. C. Slater, *Phys. Rev.* **81**, 385 (1951).
- <sup>18</sup>N. E. Christensen (unpublished) (Cu); *Phys. Status Solidi* **54**, 551 (1972) (Ag); N. E. Christensen and B. O. Seraphin, *Phys. Rev. B* **4**, 3321 (1971) (Au).
- <sup>19</sup>J. F. Janak, A. R. Williams, and V. L. Moruzzi, *Phys. Rev. B* **6**, 4367 (1972).
- <sup>20</sup>J. F. Janak, A. R. Williams, and V. L. Moruzzi, *Phys. Rev. B* **11**, 1522 (1975).
- <sup>21</sup>B. Segall and F. S. Ham, in *Methods in Computational Physics*, edited by A. Alder, S. Fernberg, and M. Rotenberg (Academic, New York, 1968), Vol. 8 Chap. 7.
- <sup>22</sup>J. C. Shaw, J. B. Ketterson, and L. R. Windmiller, *Phys. Rev. B* **5**, 3894 (1972).
- <sup>23</sup>A.-B. Chen and B. Segall, *Phys. Rev. B* **12**, 600 (1975).
- <sup>24</sup>L. Hedin and B. I. Lundqvist, *J. Phys. C* **4**, 2064 (1971).
- <sup>25</sup>Y. Glötzel, D. Glötzel, and O. K. Andersen (unpublished); see also A. R. Mackintosh and O. K. Andersen, in *Electrons at the Fermi Surface*, edited by M. Springford (Cambridge University Press, Cambridge, 1980); V. L. Moruzzi, J. F. Janak, and A. R. Williams, *Calculated Electronic Properties of Metals* (Pergamon, New York, 1978).
- <sup>26</sup>O. K. Andersen, *Phys. Rev. Lett.* **27**, 1211 (1971) and private communication.
- <sup>27</sup>O. K. Andersen, *Phys. Rev. B* **12**, 3060 (1975).
- <sup>28</sup>O. K. Andersen and O. Jepsen, *Physica (The Hague)* **91B**, 317 (1977).
- <sup>29</sup>O. Jepsen and O. K. Andersen, *Solid State Commun.* **9**, 1763 (1971); G. Lehman and M. Taut, *Phys. Status Solidi B* **54**, 469 (1972).
- <sup>30</sup>M. R. Halse, *Philos. Trans. R. Soc. London Ser. A* **265**, 507 (1969).
- <sup>31</sup>A.-B. Chen and B. Segall, *Solid State Commun.* **18**, 149 (1976).
- <sup>32</sup>D. E. Eastman and J. K. Cashion, *Phys. Rev. Lett.* **24**, 310 (1970).
- <sup>33</sup>P. O. Nilsson and B. Sandell, *Solid State Commun.* **8**, 721 (1970).
- <sup>34</sup>P. S. Wehner, R. S. Williams, S. D. Kevan, D. Denley, and D. A. Shirley, *Phys. Rev. B* **19**, 6164 (1979).
- <sup>35</sup>V. O. Kostroun, R. W. Fairchild, C. A. Kukkonen, and J. W. Wilkins, *Phys. Rev. B* **13**, 3268 (1976).
- <sup>36</sup>J. E. Muller, O. Jepsen, O. K. Andersen, and J. W. Wilkins, *Phys. Rev. Lett.* **40**, 720 (1978).
- <sup>37</sup>P. Szczepanek and R. Glosser, *Solid State Commun.* **15**, 1425 (1974).
- <sup>38</sup>P. Heiman and H. Neddermeyer, *J. Phys. F* **7**, L37 (1977).
- <sup>39</sup>N. E. Christensen, *Phys. Rev. B* (in press).